# Localization of class-related mu-rhythm desynchronization in motor imagery based Brain-Computer Interface sessions

Stefan Haufe*, Ryota Tomioka, Thorsten Dickhaus, Claudia Sannelli,
Benjamin Blankertz, Guido Nolte and Klaus-Robert Müller

***Abstract*— We localize the sources of class-dependent event-related desynchronisation (ERD) of the mu-rhythm related to different types of motor imagery in Brain-Computer Interfacing (BCI) sessions. Our approach is based on localization of single-trial Fourier coefficients using sparse basis field expansions (S-FLEX). The analysis reveals focal sources in the sensorimotor cortices, a finding which can be regarded as a proof for the expected neurophysiological origin of the BCI control signal. As a technical contribution, we extend S-FLEX to the multiple measurement case in a way that the activity of different frequency bins within the mu-band is coherently localized.**

## I. INTRODUCTION

Brain-computer interfacing aims at providing paralyzed patients a communication device that "reads thoughts" and thereby obviates the need of using the usual motor pathway. A particularly successful approach to BCI is motor imagery, i.e., a system is controlled by a user deliberately switching between movement imaginations of certain limbs. It is known that for most people the associated contralateral sensorimotor cortex becomes active already during imagination of a movement. This leads to attenuation of local sensorimotor rhythms (predominantly in the mu-range) detectable by electroencephalography (EEG); a phenomenon which is also known as event-related desynchronization (ERD) [1].

Using state-of-the-art machine learning and signal processing techniques, BCI performance has increased considerably over the last years compared to the conventional approach of extensive subject training [2]. A key ingredient for this success has been the development of algorithms that automatically adapt to the subject's individual physiology and even his/her mental strategy of performing the task (e.g. [3], [4], [5], [6]). The downside of the increased flexibility is, however, that the experimenter can no longer fully control on which features the BCI is trained. A careful examination of the extracted EEG signatures is thus required in order to draw conclusions about the physiological basis underlying a good BCI performance. Source reconstruction methods facilitate this validation as they link predictive features to the actual anatomy.

This work was supported in part by BMBF grant No. 01GQ0850, DFG grant No. MU 987/3-1 and the FP7-ICT Programme of the European Community, under the PASCAL2 Network of Excellence, ICT-216886.

S. Haufe, T. Dickhaus, C. Sannelli, B. Blankertz and K.-R. Müller are with Berlin Institute of Technology, Franklinstr. 28/29, D-10587 Berlin, Germany

R. Tomioka is with the University of Tokyo, 7-3-1 Hongo, Bunkyo-ku, Tokyo 113-8656, Japan.

G. Nolte is with Fraunhofer Institute FIRST, Kekuléstr. 7, D-12489 Berlin, Germany.

* haufe@cs.tu-berlin.de

In this paper we localize the discriminative part of the ERD occuring during different types of motor imagery, which is used as a control signal by the Berlin Brain-Computer Interface. Our approach is based on localizing raw Fourier coefficients in single trials. We deploy the recently published source reconstruction method S-FLEX [7], which is extended to deal with multiple interrelated EEG scalp patterns. This is used to co-localize all frequency patterns in the subjects' individual mu ranges, and has a noise-suppressing effect.

## II. MATERIALS AND METHODS

### A. Multiple Measurement Sparse Basis Field Expansions

Assume that the EEG activity is comprised in a single vector $\mathbf{z} = (z_1, \ldots, z_M)^\top \in \mathbb{C}^M$ containing the responses of $M$ EEG time-series to a temporal filter. Responses are assumed to take complex values here. Let $\mathbb{B} \subset \mathbb{R}^3$ be the volume covered by the brain (i.e. white and gray matter). The current density is a vector field $\mathbf{y} : \mathbb{B} \to \mathbb{C}^3$ assigning a (complex) vectorial current source to each location in the brain. Considering a discrete sample of locations (voxels) and source currents $(\mathbf{x}_n, \mathbf{y}(\mathbf{x}_n) =: \mathbf{y}_n), n = 1, \ldots, N$, we denote by $Y = (\mathbf{y}_1^\top, \ldots, \mathbf{y}_N^\top)^\top$ the $N \times 3$ matrix of sources and by $\mathbf{vec}\,(Y)$ a column vector containing the stacked transposed rows of $Y$. Instead of estimating the currents $\mathbf{y}_n$ directly, it was proposed to model the current density as a linear combination of (potentially many) spatial *basis fields*, the coefficients of which are to be estimated. We here consider an expansion into Gaussians

$$b_{n,s}(\mathbf{x}) = \left(\sqrt{2\pi}\sigma_s\right)^{-3} \exp\left(-\frac{1}{2}\left\|\mathbf{x} - \mathbf{x}_n\right\|_2^2 \sigma_s^{-2}\right) \ , \quad (1)$$

which are smooth, but also well localized due to exponentially decaying tails. Using a redundant dictionary containing Gaussians at different centers $\mathbf{x}_n$ an of different widths $s$, it has been shown that sources with arbitrary shape can be reconstructed by selecting the appropriate basis element. The respective method has been coined localization through sparse basis field expansions (S-FLEX) [7].

Given a set (*dictionary*) of basis functions $b_l, l = 1, \ldots, L$ The forward mapping from the sources $Y$ to the measurements $\mathbf{z}$ can be written in matrix form as

$$\mathbf{z} = F\,\mathbf{vec}\,(BC) \ , \quad (2)$$

using the known lead field matrix $F \in \mathbb{R}^{M \times 3N}$. Solving Eq. (2) for $C$ does not yield a unique solution if the number of coefficients is larger than the number of electrodes

$M$, which is the common situation. The ambiguity can be overcome by assuming that, for an appropriately chosen dictionary, the current density can be well approximated by a *small* number of basis fields, i.e., the coefficients are *sparse*. A natural choice for vectorial quantities is the so-called $\ell_{1,2}$-norm penalty which minimizes the (sparsity inducing) $\ell_1$-norm of the current vector *amplitudes*. The coefficients are sought which provide the best compromise between sparsity and model error, i.e.

$$\hat{C} = \arg\min_C \ \mathcal{L}(C) = \|\mathbf{z} - \Gamma\,\mathbf{vec}\,(C)\,\|_2^2 + \lambda \sum_{l=1}^{L} \|\mathbf{c}_l\|_2 \quad (3)$$

where the first and second terms are the quadratic loss function and the sparsity-inducing regularizer, respectively, $\Gamma \equiv FW(B \otimes I_{(3\times 3)}) \in \mathbb{R}^{M\times 3SN}$ and $\lambda$ is a positive constant controlling the tradeoff between loss function and regularization. Given the coefficients the estimated current density at node $\mathbf{x}_n$ is defined by

$$\hat{\mathbf{y}}_n = W_n \sum_{l=1}^{SN} \hat{\mathbf{c}}_l b_l(\mathbf{x}_n)\ . \quad (4)$$

While Eq. (3) considers only single field patterns, we would now like to extend S-FLEX to the localization of multiple measurements $\mathbf{z}(t)$. Let $Z = (\mathbf{z}(1), \ldots, \mathbf{z}(T)) \in \mathbb{C}^{M\times T}$ and $\mathbf{c}_l(t) \in \mathbb{C}^3$ be the coefficient vector describing the contribution of the $l$-th basis field to the $t$-th pattern. Defining $\mathbf{c}_l = (\mathbf{c}_l(1)^\top, \ldots, \mathbf{c}_l(T)^\top)^\top \in \mathbb{R}^{3T}$, $C = (\mathbf{c}_1, \ldots, \mathbf{c}_{SN})^\top \in \mathbb{R}^{SN\times 3T}$ and rearranging

$$\tilde{C} = \begin{pmatrix} \mathbf{c}_1(1) & \ldots & \mathbf{c}_l(T) \\ \vdots & \ddots & \vdots \\ \mathbf{c}_{SN}(1) & \ldots & \mathbf{c}_{SN}(T) \end{pmatrix} \in \mathbb{R}^{3SN\times T}\ , \quad (5)$$

we propose to estimate

$$\hat{C} = \arg\min_C \ \sum_{l=1}^{L} \|\mathbf{c}_l\|_2 + \lambda \left\| \mathbf{vec}\left(Z - \Gamma\tilde{C}\right)\right\|_2^2 \quad (6)$$

which is equivalent to Eq. (3) for $T = 1$. However, for $T > 1$ it is not equivalent to solving $T$ problems of type Eq. (3) separately, as in our case the $3T$ coefficients belonging to a certain basis function are tied under a common $\ell_2$-norm penalty and can only be pruned to zero at the same time. Thus, the selection of basis functions which contribute coherently to several patterns is facilitated, while at the same time orientations, amplitudes and phases of the corresponding fields are allowed to differ per pattern.

Minimizing the objective function Eq. (6) is a convex problem. Similar problems have been solved using second-order cone programming [8], [9], [10], [11] or iteratively reweighted least squares [12]. We here deploy a novel approach based on augmented Lagrangians, which has been proven to work for very large-scale instances [13].

*1) Effect of Joint Localization:* To illustrate the effect of co-localization, we performed the following simple experiment. A single dipolar source was placed in a cortical region of the brain and the resulting field pattern was computed. Ten different phase-shifted versions of the pattern were constructed by multiplication with a random unit-length complex number $\exp(i\phi)$. Each resulting pattern was then superimposed by equal amounts of measurement and biological noise (signal-to-noise ratio = 1.5). Note that in this scenario, the SNR cannot be increased by averaging, since both signal and noise are zero-mean complex quantities. Source localization was carried out using both the single- and multiple-measurement variants of S-FLEX, where the regularization constant was set using knowledge of the exact SNR. The source estimates of all patterns were combined to yield the estimated mean dipole amplitude.

### *B. Localizing mu-rhythm ERD during Motor Imagery*

We consider real data from experiments recently conducted within the Berlin BCI project. These experiments originally had the purpose of screening subjects with respect to BCI aptitude. The experimental protocol is described in detail in our preceding publication [14], but we here recapitulate the parts that are important for the current investigation.

Fourty healthy BCI-naive subjects (33.6 $\pm$ 13.1 years old, 22 female) participated in the study. During the experiment, they sat in a comfortable chair with arms and legs resting conveniently. EEG was acquired from 119 Ag/AgCl electrodes. In a calibration session, arrows pointing left, right or down were presented on a screen and had to be responded by five seconds of left hand, right hand or foot motor imagery, respectively. Each arrow was presented 75 times. Trials containing artifacts were discarded, as well as trials containing real limb movements (as detected by EMG). Using heuristics, well-discriminating contiguous post-stimulus time-intervals and frequency bands were identified [6].

The locations of mu-ERD generators in hand- and foot areas of the sensorimotor cortex are well known from the literature (e.g., [15], [16]). These results obtained by functional Magnetic Resonance Imaging (fMRI) serve as a hypothesis here to be confirmed by source localization. Since reliable source localization can only be expected from clean EEG signals, we restrict ourselves to cases in which EEG traces are clearly separable. That is, for each subject we are only interested in the two motor imagery classes showing best classifiability, and consider only those subjects who achieved very good BCI performance (error rates below 10%) in both the calibration and the online session. Ten subjects fell into that category. For nine of them, discriminability was found in the mu-band, as expected. A tenth subject, that achieved best BCI control using a broad band covering $\beta$- and $\gamma$-range, was excluded from the present investigation.

We apply S-FLEX to complex Fourier coefficients, which are calculated for each trial in the preselected band and pre-stimulus time interval by means of an FFT. Within the selected frequency band, five equidistantly-sampled Fourier coefficients are taken for each subject. Localization is conducted in the standard head model [17] using a source grid of $N = 6\,249$ dipoles (7mm inter-dipole distance). We consider basis functions with widths $\sigma_1 = 0.75$ cm, $\sigma_2 = 1$ cm, $\sigma_3 =$

1.25 cm and $\sigma_4 = 1.5$ cm. The regularization parameter $\lambda$ is selected by means of five-fold cross-validation, i.e. by maximizing the estimated generalization performance with respect to fitting the EEG. We use a multiple-measurement variant of S-FLEX, where all Fourier-coefficient patterns of a trial are co-localized.

## III. RESULTS

### A. Effect of Joint Localization

Results regarding the effect of joint- as compared to single-pattern localization are shown in Figure 1. It is apparent that, while both estimated source distributions peak similarly close to the true source location (indicated by a red cross-hair), the multiple-measurement approach has the advantage of being less spread-out. This shows that joint localization effectively removes the noise-induced spatial instability seen in single-trial estimates.

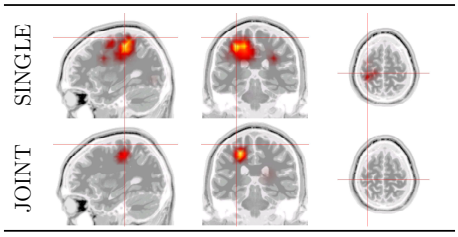


Fig. 1. Comparison of individual (SINGLE) and joint localization of ten simulated noisy measurements. The location of the true simulated source is indicated by a red cross-hair.

### B. Localizing mu-rhythm ERD during Motor Imagery

The preprocessing steps performed prior to source localization are subject-specific, i.e., include filtering in individual frequency bands, the selection of individual time intervals and class combinations, and so on. Table I lists the heuristically-chosen frequency-bands, time-intervals and the optimal class combinations for all subjects.

| SUBJECT | BAND | INTERVAL | CLASSES |
|---|---|---|---|
| *js* | 10.0 – 13.0 Hz | 1000 – 4250 ms | LEFT/RIGHT |
| *kp* | 8.0 – 12.5 Hz | 1000 – 4500 ms | LEFT/RIGHT |
| *ks* | 8.5 – 12.5 Hz | 770 – 3950 ms | LEFT/RIGHT |
| *kg* | 8.5 – 13.5 Hz | 830 – 3440 ms | LEFT/FOOT |
| *jj* | 8.5 – 13.5 Hz | 1170 – 3970 ms | LEFT/FOOT |
| *jl* | 9.5 – 13.5 Hz | 1150 – 4160 ms | LEFT/FOOT |
| *jy* | 7.5 – 11.5 Hz | 1240 – 4070 ms | LEFT/FOOT |
| *kc* | 9.5 – 13.5 Hz | 1270 – 4000 ms | LEFT/FOOT |
| *kd* | 9.5 – 13.5 Hz | 1340 – 4110 ms | LEFT/FOOT |

TABLE I
MAXIMALLY-DISCRIMINATING FREQUENCY-BANDS, TIME-INTERVALS AND OPTIMAL CLASS COMBINATIONS FOR NINE SUBJECTS.

Figure 2 allows in-depth examination of the data of one prototypical subject (subject *kp*). In the upper left part of the figure, sensor-space spectra and ERD (calculated as envelopes of the Hilbert-transformed signal) time courses at electrode C4 are shown. Gray areas mark the selected frequency-band and time-interval. Additionally, scalp maps showing classwise-averaged Band Amplitudes (BA), as well as per-channel discriminability between classes, are provided (PATTERN). Band Amplitude is defined as the $\ell_2$-norm of the vector of Fourier-coefficients in the heuristically selected frequency band, while discriminability is measured in terms of the signed $r^2$-value, which is defined as the signed squared biserial correlation coefficient between class label and Band Amplitude.

Source maps obtained from localizing Fourier coefficient patterns are presented in the lower part of Figure 2 (LOCALIZATION). These maps can be regarded as the source-space equivalents of the scalp maps depicted in the panel PATTERN. Voxel-wise Band Amplitude in source space is defined as in sensor-space, but it is accounted for that in source space three Fourier-coefficients exist per voxel and frequency. Discriminability in source space is measured in terms of a weighted signed $r^2$-value, where the discriminability index at each voxel is normalized by the average Band Amplitude at this voxel (taken over trials of both classes). This is done in order to suppress high $r^2$-values at locations with negligible estimated activity, which are otherwise observed as a result of the sparsity of the S-FLEX solution.

The $r^2$ scalp map of subject *kp* shows strong (opposing) contralateral ERD effects for left and right hand conditions, which are maximal around C3 and C4, respectively. Classwise-averaged maps of source activity as estimated from Fourier coefficients show distinguished blobs in left/right hand areas within the sensorimotor cortex for both subjects. More such blobs are observed in other cortical regions, in particular in frontal and occipital lobes. However, in accordance with our expectation and the sensor-space plots, these sources cancel out as being nondiscriminative, and only hand areas remain in the source $r^2$-maps.

Figure 3 provides source-space discriminablity maps for the rest of the nine subjects considered. These plots generally resemble those of either subject *kp*. For subjects *js* and *ks*, having the optimal class combination LEFT vs. RIGHT, the same opposing contralateral activation of hand areas as in subject *kp* is observed. The rest of the subjects utilize foot imagery, although a clear desynchronization in the central somatosensory cortex during that condition is only found in subject *jl*. In the left hand condition, all these subjects exhibit desynchronization of both hand areas simultaneously. This supports the hypothesis that the foot condition often serves as a pseudo class, and some subjects may effectively achieve one-dimensional BCI control utilizing only the presence or absence of (left *and* right) hand-related ERD.

## IV. CONCLUSION

The localization results obtained here confirm that the features that discriminate best between different types of motor imagery are spectral differences in corresponding parts of the sensorimotor cortex. This is in agreement with [18]

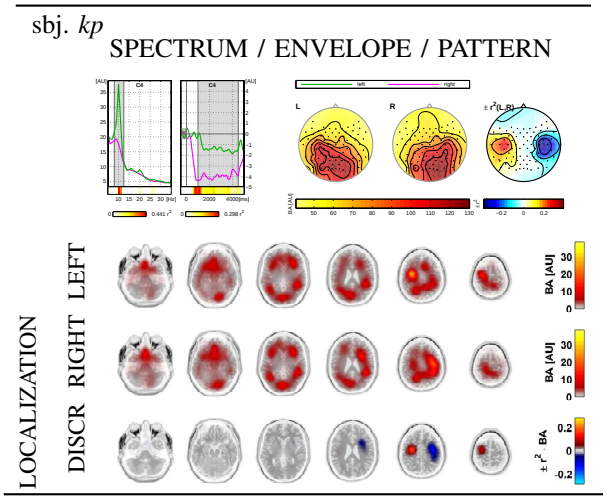


Fig. 2. Results for subject *kp*: Event-related desynchronization (ERD) occurring during LEFT and RIGHT hand motor imagery conditions. Upper part: Average poststimulus amplitude spectrum (SPECTRUM) and time course (ENVELOPE) at C4. PATTERN: Average topographical Band Amplitude plots for single conditions, as well as signed $r^2$ measure of discriminability between conditions. LOCALIZATION: S-FLEX estimated source distributions (Band Amplitude) for LEFT and RIGHT hand conditions, as well as discriminability (DISCR) between conditions.

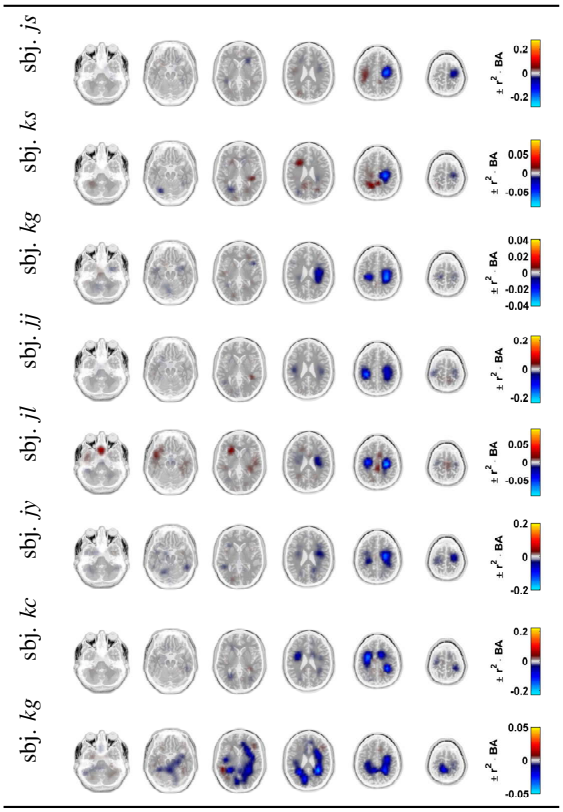


Fig. 3. S-FLEX source-space discriminability between best (discriminating) conditions for eight subjects. Source estimates are obtained from single-trial localization of Fourier-coefficients. For subjects *js* and *ks* the optimal conditions are left and right hand imagery, while for all other subjects the optimal combination is left hand vs. foot imagery.

and previous fMRI studies. The present study hence serves as a validation of neurophysiological significance of the Berlin BCI feature extraction. The obtained separability in source space raises the question whether source reconstruction methods can also be used to improve BCI accuracy.

## REFERENCES


[1] G. Pfurtscheller and F. H. L. da Silva, "Event-related EEG/MEG synchronization and desynchronization: basic principles," vol. 110, no. 11, pp. 1842–1857, Nov 1999.

[2] G. Dornhege, J. d. R. Millán, T. Hinterberger, D. McFarland, and K.-R. Müller, Eds., *Toward Brain-Computer Interfacing.* Cambridge, MA: MIT Press, 2007.

[3] C. Vidaurre, A. Schlögl, R. Cabeza, R. Scherer, and G. Pfurtscheller, "A fully on-line adaptive BCI," *IEEE Trans Biomed Eng*, vol. 53, pp. 1214–1219, Jun 2006.

[4] K.-R. Müller, M. Tangermann, G. Dornhege, M. Krauledat, G. Curio, and B. Blankertz, "Machine learning for real-time single-trial EEG-analysis: From brain-computer interfacing to mental state monitoring." *J. Neurosci. Meth.*, vol. 176, pp. 82–90, 2008.

[5] B. Blankertz, G. Dornhege, M. Krauledat, K.-R. Müller, and G. Curio, "The non-invasive Berlin Brain-Computer Interface: Fast acquisition of effective performance in untrained subjects," *NeuroImage*, vol. 37, no. 2, pp. 539–550, 2007.

[6] B. Blankertz, R. Tomioka, S. Lemm, M. Kawanabe, and K.-R. Müller, "Optimizing spatial filters for robust EEG single-trial analysis," *IEEE Signal Proc. Magazine*, vol. 25, pp. 41–56, 2008.

[7] S. Haufe, V. V. Nikulin, A. Ziehe, K.-R. Müller, and G. Nolte, "Estimating vector fields using sparse basis field expansions," in *Advances in Neural Information Processing Systems 21*, D. Koller, D. Schuurmans, Y. Bengio, and L. Bottou, Eds. Cambridge, MA: MIT Press, 2009, pp. 617–624.

[8] S. Haufe, V. V. Nikulin, A. Ziehe, K.-R. Müller, and G. Nolte, "Combining sparsity and rotational invariance in EEG/MEG source reconstruction," *NeuroImage*, vol. 42, no. 2, pp. 726–738, 2008.

[9] D. Malioutov, M. Çetin, and A. S. Willsky, "A sparse signal reconstruction perspective for source localization with sensor arrays," *IEEE Trans. Signal Proces.*, vol. 55, no. 8, pp. 3010–3022, 2005.

[10] W. Ou, M. S. Hämäläinen, and P. Golland, "A distributed spatio-temporal EEG/MEG inverse solver," *NeuroImage*, vol. 44, pp. 932–946, 2008.

[11] L. Ding and B. He, "Sparse source imaging in EEG with accurate field modeling," *Hum. Brain Mapp.*, vol. 29, no. 9, pp. 1053–1067, 2008.

[12] D. Wipf and B. Rao, "An empirical bayesian strategy for solving the simultaneous sparse approximation problem," *IEEE Trans. Signal Proces.*, vol. 55, no. 7, pp. 3704–3716, 2007.

[13] R. Tomioka and M. Sugiyama, "Dual augumented lagrangian method for efficient sparse reconstruction," *IEEE Signal Proc. Let.*, vol. 16, no. 2, pp. 1067–1070, 2009.

[14] B. Blankertz, C. Sannelli, S. Halder, E. M. Hammer, A. Kübler, K. R. Müller, G. Curio, and T. Dickhaus, "Neurophysiological predictor of SMR-based BCI performance," *NeuroImage*, vol. 51, pp. 1303–1309, Jul 2010.

[15] M. Leonardo, J. Fieldman, N. Sadato, G. Campbell, V. Ibanez, L. Cohen, M. P. Deiber, P. Jezzard, T. Pons, R. Turner, D. L. Bihan, and M. Hallett, "A functional magnetic-resonance-imaging study of cortical regions associated with motor task execution and motor ideation in humans," *Hum. Brain Mapp.*, vol. 3, pp. 83–92, 1995.

[16] C. A. Porro, M. P. Francescato, V. Cettolo, M. E. Diamond, P. Baraldi, C. Zuiani, M. Bazzochi, and P. di Prampero, "Primary motor and sensory cortex activation during motor performance and motor imagery: A functional magnetic resonance imaging study," *J. Neurosci.*, vol. 16, pp. 7688–7698, 1996.

[17] C. J. Holmes, R. Hoge, L. Collins, R. Woods, A. W. Toga, and A. C. Evans, "Enhancement of MR images using registration for signal averaging," *J. Comput. Assist. Tomogr.*, vol. 22, no. 2, pp. 324–333, 1998.

[18] H. Yuan, A. Doud, A. Gururajan, and B. He, "Cortical imaging of event-related (de)synchronization during online control of brain-computer interface using minimum-norm estimates in the frequency domain," *IEEE Trans. Neural. Syst. Rehabil. Eng.*, vol. 16, pp. 425–431, 2008.